From nonwetting to prewetting: The asymptotic behavior of ^{4}He drops on alkali substrates

M. Barranco,[1] M. Guilleumas,[1] E. S. Hernández,[2] R. Mayol,[1] M. Pi,[1] and L. Szybisz[2,3]
[1]*Departament ECM, Facultat de Física, Universitat de Barcelona, E-08028 Barcelona, Spain*
[2]*Departamento de Física, Facultad de Ciencias Exactas y Naturales, Universidad de Buenos Aires, 1428 Buenos Aires, Argentina and Consejo Nacional de Investigaciones Científicas y Técnicas, Buenos Aires, Argentina*
[3]*Departamento de Física, CAC, Comisión Nacional de Energía Atómica, 1429 Buenos Aires, Argentina*
(Received 18 March 2003; published 28 July 2003)

We investigate the spreading of ^{4}He droplets on alkali-metal surfaces at zero temperature, within the frame of finite range density-functional theory. The equilibrium configurations of several ^4He_N clusters and their asymptotic trend with increasing particle number N, which can be traced to the wetting behavior of the quantum fluid, are examined for nanoscopic droplets. We discuss the size effects inferring that the asymptotic properties of large droplets correspond to those of the prewetting film.

DOI: 10.1103/PhysRevB.68.024515 PACS number(s): 67.60.−g, 67.70.+n, 61.46.+w

I. INTRODUCTION

Wetting phenomena[1,2] of alkali-metal and graphite-based surfaces by quantum fluids have been a burgeoning field of research in recent years, both from the experimental and the theoretical viewpoints. Early in the last decade, it was demonstrated that liquid ^{4}He is not a universal wetting agent,[3–9] since it fails to spread uniformly on cesium surfaces at temperatures below 1.95 K. From the theoretical viewpoint, Cheng *et al.*[10] predicted, in the frame of a nonlocal density-functional model, the inability of helium to wet all heavy alkalimetals. More stringent theoretical studies[11–15] showed that while for the majority of moderately thin to thick helium films on substrates, one or two layers of solid helium would be continuously wetted by the excess liquid, a different pattern was to be expected in the presence of weak adsorbers. In this case, either nonwetting or wetting preceded by a first-order prewetting transition,[16] was most likely to appear. The prewetting transition undergone by ^{4}He on Cs substrates was first observed by Hallock and co-workers[7] and the complete phase diagram was presented in Ref. 8. The situation is not so clear for Rb surfaces, since although a number of experimental evidences[5,17] and at least one theoretical calculation[18] are consistent with a vanishing wetting temperature, a more recent experiment[19] indicates that pristine Rb is nonwetted by helium up to a temperature above 300 mK, in agreement with earlier predictions.[20,21]

So far, theoretical work on wetting properties of helium relies almost exclusively on the description of structure and energetics of films, uniformly extended on the plane perpendicular to the substrate, in spite that all these systems, even on wetted substrates, are thermodynamically unstable for the lowest areal coverages and should then appear as collections of puddles or clusters upon the adsorbing surface.[2] In a prior work, Ancilotto *et al.*[22] have presented a calculation of density profiles of finite droplets of ^{4}He on Cs, at zero temperature. These authors solve a nonlinear equation for the density profile, constructed by functional differentiation of a finite range density functional (FRDF) acknowledged as the Orsay-Trento (OT) density functional.[23] Quite elaborated from the numerical viewpoint, this work develops an accurate theoretical instrument to investigate wetting patterns.

The purpose of this work is to perform a detailed investigation of the spreading of ^{4}He droplets on alkali-metal surfaces at zero temperature in the framework of the FRDF formalism. Our systematic study permits us to relate the asymptotic trends of their energetics and structure, with increasing size, to the wetting properties of the fluid; in particular, we show that droplets as large as a few thousand ^{4}He atoms, on the strongest adsorbers, already exhibit the structural and thermodynamic characteristics of the prewetting film at zero temperature.

In Sec. II, we shortly review the current FRDF formulation and give essential details of the method applied to solving the associated Euler-Lagrange (EL) equation to obtain the equilibrium configuration. In Sec. III, we illustrate the predicted prewetting transition for films on alkali-metal adsorbers, and subsequently, we present the numerical results for clusters. Our conclusions and perspectives are presented in Sec. IV.

II. DENSITY-FUNCTIONAL DESCRIPTION OF ^{4}He CLUSTERS ON ADSORBING SUBSTRATES

The FRDF for ^{4}He adopted in this work is that of Ref. 24, which was originally developed to describe mixtures of helium isotopes, here restricted to the ^{4}He component. Its detailed form and values of the coefficients entering its definition have been given in Ref. 25, with the two changes reported in Ref. 24 which consist, on the one hand, in the neglect of the nonlocal gradient correction to the kinetic-energy term in Ref. 23, and on the other hand, in the choice of the suppressed Lennard-Jones core as in Ref. 26, namely,

$$V_{LJ}(r)=\begin{cases} 4\varepsilon[(\sigma_4/r)^{12}-(\sigma_4/r)^6] & \text{if } r\geqslant h \\ V_0(r/h)^4 & \text{if } r\leqslant h, \end{cases} \tag{1}$$

with $\varepsilon=10.22$ K, $\sigma_4=2.556$ Å, and with hard-core radius $h=2.359\,665$ Å. Notice that V_0 is the value of the 6-12 potential at $r=h$. The value of h has been fixed so that the volume integral of the interaction V_{LJ} coincides with the one in Refs. 23 and 25. This form of the FRDF has been introduced to render the numerical calculations less cumbersome—we especially comment that our FRDF yields

TABLE I. Energy $\mathcal{E}_4$ (K) of one ^{4}He atom on different alkali-metal substrates.

Li	Na	K	Rb	Cs
−10.70	−7.08	−4.20	−3.72	−3.53

a surface tension for ^{4}He of 0.282 K Å^{-2} instead of the commonly accepted experimental value ~0.272 –0.275 K Å^{-2}.[27,28]

The integrodifferential EL equation arising from functional differentiation of the FRDF is

$$\left[-\frac{\hbar^2}{2m_4}\nabla^2+V(\rho)\right]\Psi(\mathbf{r})\equiv\mathcal{H}_H\Psi(\mathbf{r})=\mu\Psi(\mathbf{r}), \qquad (2)$$

with μ the chemical potential that enforces particle number N conservation in the drop, and with $\Psi=\sqrt{\rho}$, where $\rho(\mathbf{r})$ is the particle density. The mean field $V(\mathbf{r})$ in the Hartree Hamiltonian $\mathcal{H}_H$ includes the potential $V_s(z)$ generated by the alkali-metal substrate filling the $z\leqslant 0$ half space. For $z\geqslant 0$, $V_s(z)$ is chosen to be the appropriate Chizmeshya-Cole-Zaremba (CCZ) potential.[20] To illustrate the adsorbing power of the alkali-metal surfaces, in Table I, we show the energies $\mathcal{E}_4$ of one ^{4}He atom in the substrate, obtained with the CCZ potentials.

In the current geometry, for axially symmetric droplets, we have $\rho(\mathbf{r})=\rho(r,z)$. The EL equation is discretized using seven-point formulas and solved on a two-dimensional (r,z) cylindrical mesh. We have used a sufficiently large box with spatial steps $\Delta r=\Delta z\equiv\Delta=h/12\sim 0.197$ Å. The stability of our results against the increase of the number of mesh points, as well as with respect to the order of the formulas employed to discretize the partial derivatives, has been checked comparing the solutions for spherical drops with those obtained with a spherically symmetric code. We have employed an imaginary time method to find the forward solution of the imaginary time diffusion equation[29]

$$\frac{\partial\Psi}{\partial\tau}=-(\mathcal{H}_H-\mu)\Psi, \qquad (3)$$

in other words,

$$\Psi(\tau+\delta\tau)-\Psi(\tau)\equiv\Delta\Psi(\tau)=-\delta\tau(\mathcal{H}_H-\mu)\Psi(\tau), \quad (4)$$

where $\mu=\langle\Psi(\tau)|\mathcal{H}_H|\Psi(\tau)\rangle$.

To accelerate the self-consistent solution of this equation, we use the preconditioning smoothing operation described in Ref. 30. This means that $\Delta\Psi(\tau)$ has been smoothed as

$$\overline{\Delta\Psi}(r,z;\tau)=\frac{1}{2}\Big\{\Delta\Psi(r,z;\tau)+\frac{1}{4}[\Delta\Psi(r-\Delta r,z;\tau)+\Delta\Psi(r+\Delta r,z;\tau)+\Delta\Psi(r,z-\Delta z;\tau)+\Delta\Psi(r,z+\Delta z;\tau)]\Big\}. \qquad (5)$$

Finally, the perfomance of the code has been further improved by adding a ''viscosity term,'' i.e., Eq. (4) has been changed into

$$\Psi(\tau+\delta\tau)=\Psi(\tau)+\overline{\Delta\Psi(\tau)}+\alpha_V[\Psi(\tau)-\Psi(\tau-\delta\tau)]. \qquad (6)$$

The heuristic viscosity parameter α_V is fixed to a value of 0.8.

We recall that as shown in Ref. 29, the maximum τ step, $\delta\tau_m$, that can be used to produce a stable imaginary time evolution is $\hbar^2\delta\tau_m/(2m_4\Delta^2)\lesssim 1/4$. The combination of smoothing and viscosity allows one to use large values of $\delta\tau$, typically up to $\delta\tau\sim 0.5\,\delta\tau_m$. After every τ step, the ^{4}He density is normalized to N. The iteration procedure starts on the halved density of a $^4\mathrm{He}_{2N}$ cluster calculated with the spherically symmetric code. Most of the computational time is spent in the evaluation of the mean field $V(r,z)$ by folding the helium density with the screened Lennard-Jones potential. For this reason, the mean field is updated only every ten τ iterations.

III. EQUILIBRIUM CONFIGURATIONS

A. Films

The thermodynamic criterion for wetting requests that the surface grandpotential, namely, at zero temperature $\sigma=(E-\mu N)/A$, where A is the area of the surface, regarded as a function of coverage $n=N/A$, displays its absolute minimum when n approaches infinity.[11,14] For films of ^{4}He, and within the density-functional frame,[18] this criterion can be formulated in terms of the expansion coefficients of the total energy of the film in powers of $1/n$. In particular, it has been shown that the OT density functional plus the CCZ potential yields, for ^{4}He films on alkali-metal substrates, wetting of Rb[18] and K,[31] and nonwetting of a Cs surface.[34] In Figs. 1 and 2, we, respectively, plot the chemical potential and the surface grandpotential of ^{4}He on different alkali-metal surfaces, as predicted by the current FRDF. The energy per particle $e=E/N$ that corresponds to the equilibrium density for a given coverage is also shown in Fig. 1 in dashed lines for Cs, Na, and Li.

It is worthwhile to recall here that from the thermodynamic relations

$$\mu=e+n\frac{\partial e}{\partial n}, \qquad (7)$$

$$\sigma=-n^2\frac{\partial e}{\partial n}=\int_0^n dn'[\mu(n')-\mu(n)], \qquad (8)$$

one can establish the condition $\mu=e$ to localize the prewetting jump. This condition corresponds to vanishing areal grandpotential

$$\frac{\partial e}{\partial n}=\sigma=0, \qquad (9)$$

from where the Maxwell construction (8) defines the chemical potential and coverage at the prewetting first-order tran-

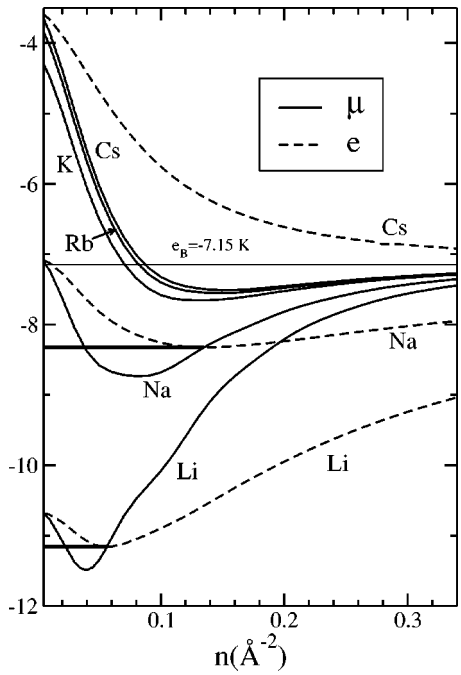

FIG. 1. Chemical potential μ (K) of ^{4}He atoms in films upon Cs, Rb, K, Na, and Li substrates as functions of areal coverage n (Å^{-2}), predicted by the FRDF employed in this work. Also shown is the energy per particle e (K) for Cs, Na, and Li, and the energy per particle in bulk ^{4}He e_B as a straight line.

sition. The prewetting jumps are indicated in Fig. 1 as horizontal segments, for the stronger adsorbers Na and Li. Although K is wetted by helium in the current FRDF description (see Fig. 3), the prewetting jump lies too far to the right in the scale here displayed. In the present calculation, ^{4}He does not wet Rb and behaves very much like Cs; this can be appreciated in Fig. 3 where the surface grandpotential of the film is plotted as a function of the inverse coverage.[32]

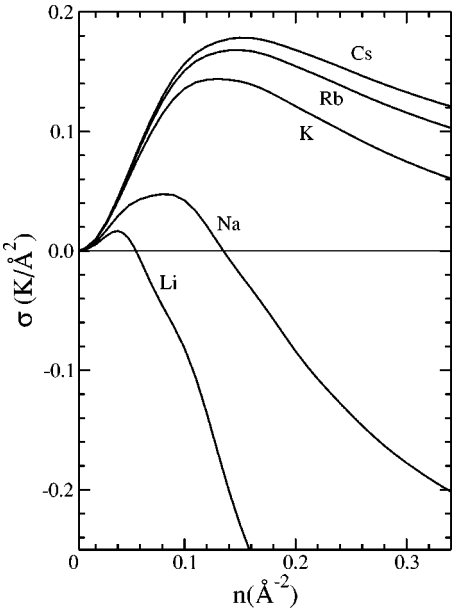

FIG. 2. Same as Fig. 1 for the surface grandpotential.

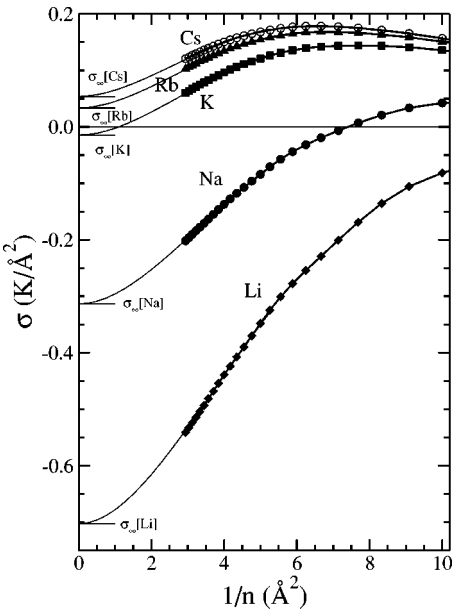

FIG. 3. Surface grandpotential as a function of inverse coverage. The short horizontal line near $1/n=0$ represents the value of the surface grandpotential in the limit of infinite coverage.

Indeed, it has been already pointed out that this substrate represents a delicate limiting case, largely sensitive to the details of the calculation, of the density functional and of the adsorbing potential adopted.[18,21,34]

B. Clusters

We concentrate on droplet sizes below $N=3000$, which illustrate the spreading trend on adsorbers of different strengths and provide a good representation of the asymptotic behavior as shown below. Addressing larger drops requires larger mesh sizes, which is possible at the obvious price of making the calculations more cumbersome and time consuming. In Fig. 4, we show the contour plots of the particle densities in the (x,z) plane for a cluster with $N=1000$, on substrates of Cs, K, Na, and Li—Rb looks very much as Cs, and for this reason we do not discuss it here. The profiles $\rho(r,z_{min})$ of these drops, at the minimum z_{min} of the CCZ potential, and $\rho(0,z)$ along the symmetry axis are plotted in Fig. 5 for the same substrates (note r is in the xy plane). As we see, increasing attractiveness provokes a change of shape in two complementary manners, which becomes most noticeable for the clusters on Na and Li, i.e., flattening along the vertical coordinate, and sizable radial spreading. We also visualize a smoothing of the structure, since the oscillations in $\rho(0,z)$ evolve from practically three peaks on Cs and K, and two on Na, to just one on Li. This feature does reflect the wetting behavior obtained for ^{4}He on these alkali-metals, namely, nonwetting for Cs and prewetting with a jump of above three layers on K, two on Na, and one on Li, respectively. In fact, submonolayer wetting occurs for the strongest adsorber Li.[14,15,35]

The energetics as a function of cluster size is illustrated in Fig. 6, where we plot the chemical potential of the ^{4}He atoms and the grandpotential per particle $\omega=E/N-\mu$ as func-

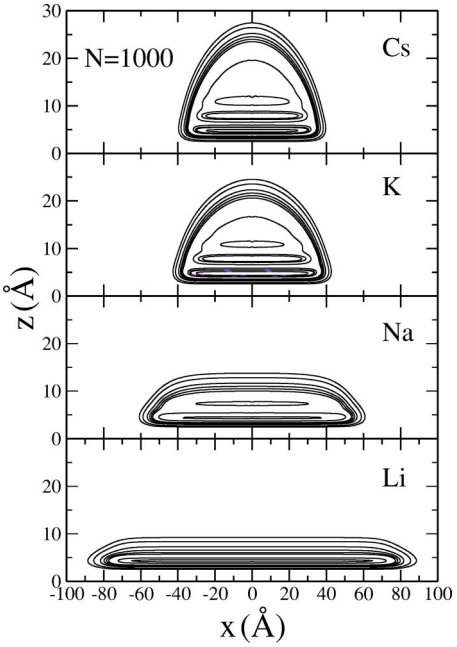

FIG. 4. Contour plot of the density of a $^4He_{1000}$ droplet on Cs, K, Na, and Li. For Li, the equidensity lines correspond to $\rho = 10^{-4}$, 5×10^{-4}, 2.5×10^{-3}, 5×10^{-3}, 7.5×10^{-3}, 10^{-2}, 2×10^{-2}, and 2.5×10^{-2} Å^{-3}; for Na, to the same values as for Li but with 3×10^{-2} instead of 2.5×10^{-2}; and for Cs and K, to the same values as for Li and Na up to $\rho=2\times10^{-2}$, with additional equidensity lines corresponding to $\rho=2.2\times10^{-2}$, 2.3×10^{-2}, and 2.6×10^{-2} Å^{-3}.

tions of N for the above alkali-metals. From this figure, we realize that for wetted adsorbers, there is a tendency—very clear for the strongest substrates Na and Li—to saturate μ at a finite value below the bulk value -7.15 K and ω at zero value. In the case of Cs, the limiting chemical potential

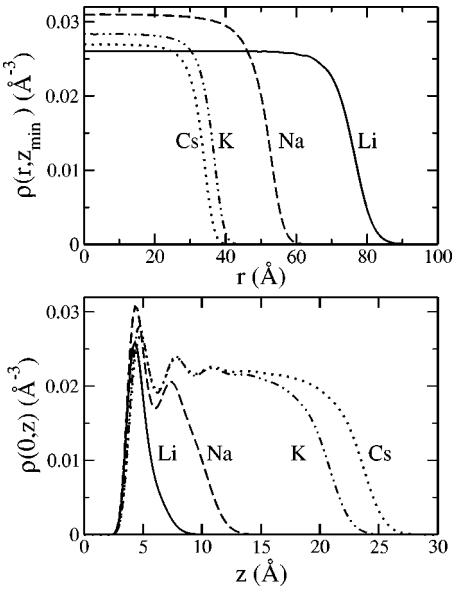

FIG. 5. Density profiles $\rho(r,z_{min})$ (upper panel) and $\rho(0,z)$ (lower panel) of a $^4He_{1000}$ cluster on different alkali-metal substrates.

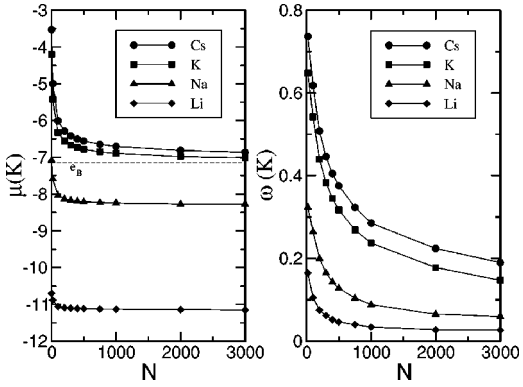

FIG. 6. Chemical potential (left panel) and grandpotential per particle (right panel) of ^{4}He droplets on alkali-metal adsorbers as a function of N. The energy per particle in bulk ^{4}He e_B is also shown in the left panel. The lines have been drawn to guide the eye.

points towards the bulk figure, in agreement with the non-wetting behavior of ^{4}He; notice that although ^{4}He wets K, as seen in Fig. 3, within the current scale we do not reach values of μ lower than -7.15 K, since this crossing takes place at a much larger number of atoms, likely several tens of thousands.

We now select Na as a test case to examine the evolution of the density profiles with particle number; as a reference, in Fig. 7 we depict the contour plots of the particle densities in the (x,z) plane for several values of N varying between 100 and 3000, where we already observe a rather flat profile with two ridges, corresponding to density oscillations parallel to the substrate. Figure 8 displays $\rho(r,z_{min})$ and $\rho(0,z)$ for the above particle numbers. We appreciate a definite inclination to saturate the vertical density profiles with two shells and a

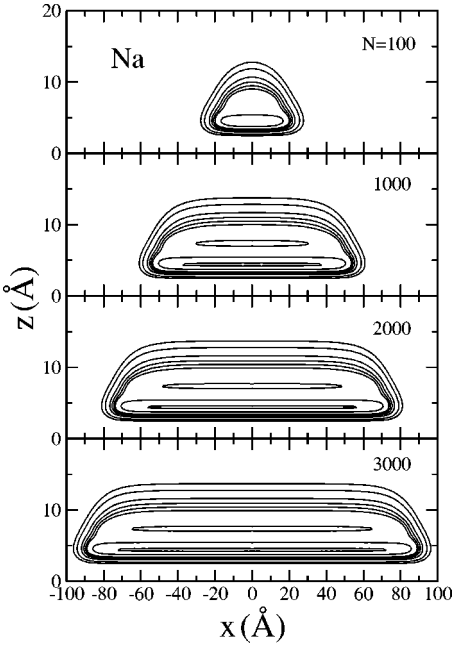

FIG. 7. Contour plots of the density of a ^4He_N droplet on Na for $N=100$, 1000, 2000, and 3000. The equidensity lines are as in Fig. 4 for Na.

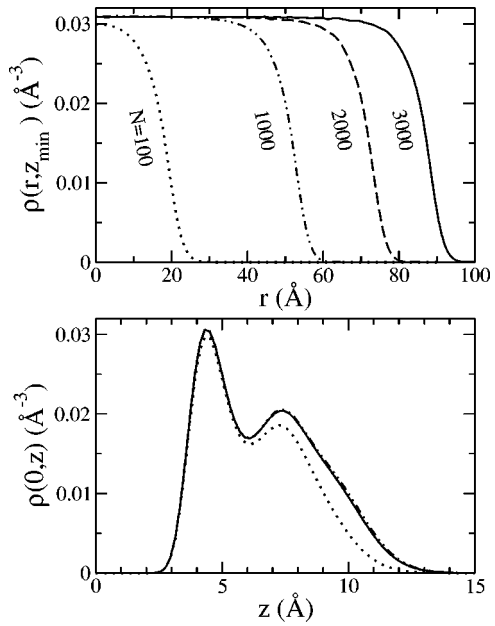

FIG. 8. Density profiles $\rho(r,z_{min})$ (upper panel) and $\rho(0,z)$ (lower panel) of ^4He_N clusters on Na.

limiting height, as well as a tendency to flatten the radial dependence into a wedgelike shape, forcing outwards any extra material. These effects are more pronounced in the case Li, as can be seen from Fig. 9 where the submonolayer profiles become manifest; nevertheless, it should be kept in mind that as mentioned in Ref. 35, density-functional theory predicts a prewetting jump at a larger coverage than, i.e., path-integral Monte Carlo calculations.

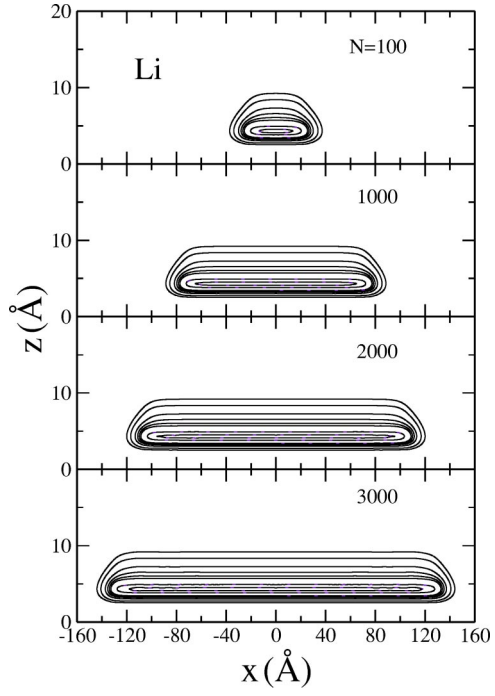

FIG. 9. Contour plots of the density of a ^4He_N droplet on Li for $N=100$, 1000, 2000, and 3000. The equidensity lines are as in Fig. 4 for Li.

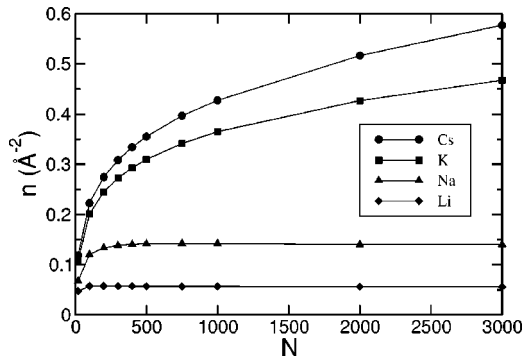

FIG. 10. Coverage $n(r=0)$ for ^4He_N droplets on the various alkali-metal substrates as a function of number of atoms. The lines have been drawn to guide the eye.

These patterns suggest the existence of an asymptotic coverage at the center of large clusters; in fact, as we define

$$n(r)=2\pi\int dz\rho(r,z), \tag{10}$$

and plot $n(0)$ as a function of N for all substrates under consideration as shown in Fig. 10, the shapes of these curves indicate that for wetted adsorbers such an asymptotic value exists. Our data indicate that these limiting numbers are $[\mu_{Na},n_{Na}(0)]=(-8.27\ \mathrm{K},0.14\ \mathrm{Å}^{-2})$ and $[\mu_{Li},n_{Li}(0)]=(-11.15\ \mathrm{K},0.06\ \mathrm{Å}^{-2})$. These values coincide with the coordinates of the respective prewetting points shown on the curves for the chemical potentials displayed in Fig. 1.

IV. SUMMARY AND OUTLOOK

In this work, we have described the spreading of ^4He droplets on alkali-metal subtrates as they grow in size. One outcome of this investigation is that for wetted substrates, the large size limit is not the bulk liquid but, interestingly, the minimum stable film. In other words, the deposited cluster can grow towards the thermodynamic limit along the directions permitted by the geometrical constraint, namely, those parallel to the planar substrate. The transverse extent just fixes the maximum height of the sample so as to yield the prewetting coverage.

Along this work, we have shown density profiles of clusters on alkali-metal adsorbers, and seen that for wetted substrates, droplets of ^4He atoms are present in the nonwetting, subspinodal regime—i.e., $\partial\mu/\partial n<0$—and seem to present a contact angle in spite that, in the light of the results discussed in the preceding section, the asymptotic limit of these large systems is the prewetting film that is associated with vanishing contact angle. This apparent inconsistency stems from the impossibility to define a contact angle for nanoscopic droplets in which the particle density displays a nonnegligible surface width, and is highly stratified near the substrate, which render the contact angle an ill-defined quantity. It also illustrates that a determination of the contact angle by visual inspection of the equidensity lines is fraught with danger and may lead to either a crude estimate or even to a qualitatively wrong result. As we have commented, Ancilotto

et al.[22] presented density profiles of ^{4}He droplets on Cs, at zero temperature, for the OT density functional.[23] In this work, emphasis lay on the determination of the contact angle of macroscopic nonwetting samples of ^{4}He on Cs, and a rather complex procedure was developed that permitted to compute this angle extrapolating the results for nanoscopic drops to the macroscopic ones for which a contact angle can be sensibly defined. We want to point out that since the FRDF here employed differs only slightly from the OT—we have verified that no visible discrepancies show up in the structural properties of clusters on Cs—applying the method of Ref. 22 would yield in our case a similar contact angle for ^{4}He on Cs (about 36°, cf. Table I in Ref. 34).

An interesting extension of this work is the investigation of the spreading of mixed ^{3}He-^{4}He clusters on planar substrates. Such a project is feasible within the FRDF formalism, and in fact, we have recently shown[36] that one or few ^{3}He atoms added to a large—yet nanoscopic—^{4}He drop on Cs, localize on a one-dimensional ring around the contact line. This is a new feature of helium mixtures, which may contribute to interpreting the very complex phase diagram of such systems.[37] A detailed systematics of the structure and energetics of mixed clusters is presently in progress and will be reported elsewhere.

Finally, we would like to mention that the FRDF formalism may also be used to shed light on the nucleation of wetting layers in the case of a first-order wetting transition, very much as it has been successfully used to address nucleation or cavitation in bulk liquid helium.[38] A major advantage of the formalism is that it may circumvent some of the approximations made in other approaches. In particular, it avoids the use of an experimentally unknown line tension[39] and the use of a separation between surface and line contributions to the free energy,[40] which becomes doubtful when the radius of the critical droplet or bubble is comparable to its surface width.

ACKNOWLEDGMENTS

This work has been performed under Grants Nos. BFM2002-01868 from DGI, Spain, 2001SGR-00064 from Generalitat of Catalonia, EX-130 from University of Buenos Aires, and PICT2000-03-08450 from ANPCYT, Argentina. E.S.H. has been also funded by M.E.C.D. (Spain) on sabbatical leave. We are grateful to Francesco Ancilotto and to Milton Cole for useful discussions.

[1] P.G. de Gennes, Rev. Mod. Phys. **57**, 827 (1985).
[2] D. Bonn and D. Ross, Rep. Prog. Phys. **64**, 1085 (2001).
[3] P.J. Nacher and J. Dupont-Roc, Phys. Rev. Lett. **67**, 2966 (1991).
[4] P. Taborek and J. Rutledge, Phys. Rev. Lett. **68**, 2184 (1992).
[5] N. Bigelow, P.J. Nacher, and J. Dupont-Roc, J. Low Temp. Phys. **89**, 135 (1992).
[6] S.K. Mukherjee, D.P. Drusit, and M.H.W. Chan, J. Low Temp. Phys. **97**, 113 (1992).
[7] K.S. Ketola, S. Wang, and R.B. Hallock, Phys. Rev. Lett. **68**, 201 (1992).
[8] J.E. Rutledge and P. Taborek, Phys. Rev. Lett. **69**, 937 (1992).
[9] P. Taborek and J. Rutledge, Physica B **197**, 283 (1994).
[10] E. Cheng, M.W. Cole, W.F. Saam, and J. Treiner, Phys. Rev. Lett. **67**, 1007 (1991).
[11] E. Cheng, M.W. Cole, W.F. Saam, and J. Treiner, Phys. Rev. B **46**, 13 967 (1992).
[12] E. Cheng, M.W. Cole, W.F. Saam, and J. Treiner, J. Low Temp. Phys. **89**, 657 (1992).
[13] W.F. Saam, J. Treiner, E. Cheng, and M.W. Cole, J. Low Temp. Phys. **89**, 637 (1992).
[14] E. Cheng, M.W. Cole, J. Dupont-Roc, W.F. Saam, and J. Treiner, Rev. Mod. Phys. **65**, 557 (1993).
[15] B.E. Clements, H. Forbert, E. Krotscheck, and M. Saarela, J. Low Temp. Phys. **85**, 849 (1994).
[16] J.W. Cahn, J. Chem. Phys. **66**, 3667 (1977); C. Ebner and W.F. Saam, Phys. Rev. Lett. **38**, 1486 (1977).
[17] G. Mistura, H.C. Lee, and M.H.W. Chan, Physica B **194-196**, 661 (1994); B. Demolder, N. Bigelow, P.J. Nacher, and J. Dupont-Roc, J. Low Temp. Phys. **98**, 91 (1995); A.F.G. Wyatt, J. Klier, and P. Stefanyi, Phys. Rev. Lett. **74**, 1151 (1995); T.A. Moreau and R.B. Hallock, J. Low Temp. Phys. **110**, 65 (1998); J.A. Phillips, D. Ross, P. Taborek, and J.E. Rutledge, Phys. Rev. B **58**, 3361 (1998).
[18] L. Szybisz, Phys. Rev. B **62**, 12 381 (2000).
[19] J. Klier and A. Wyatt, Phys. Rev. B **65**, 212504 (2002).
[20] A. Chizmeshya, M.W. Cole, and E. Zaremba, J. Low Temp. Phys. **110**, 677 (1998).
[21] F. Ancilotto, F. Faccin, and F. Toigo, Phys. Rev. B **62**, 17 035 (2000).
[22] F. Ancilotto, A.M. Sartori, and F. Toigo, Phys. Rev. B **58**, 5085 (1998).
[23] F. Dalfovo, A. Lastri, L. Pricaupenko, S. Stringari, and J. Treiner, Phys. Rev. B **52**, 1193 (1995).
[24] R. Mayol, M. Pi, M. Barranco, and F. Dalfovo, Phys. Rev. Lett. **87**, 145301 (2001).
[25] M. Barranco, M. Pi, S.M. Gatica, E.S. Hernández, and J. Navarro, Phys. Rev. B **56**, 8997 (1997).
[26] J. Dupont-Roc, M. Himbert, N. Pavloff and J. Treiner, J. Low Temp. Phys. **81**, 31 (1990).
[27] H.M. Guo, D.O. Edwards, R.E. Sarwinski, and J.T. Tough, Phys. Rev. Lett. **27**, 1259 (1971).
[28] G. Deville, P. Roche, N.J. Appleyard, and F.I.B. Williams, Czech. J. Phys. **46**, 89 (1996).
[29] W.H. Press, S.A. Teukolsky, W.T. Vetterling, and B.P. Flannery, *Numerical Recipies* (Cambridge University Press, Cambridge, 1992).
[30] T. Hoshi, M. Arai, and T. Fujiwara, Phys. Rev. B **52**, R5459 (1995).
[31] L. Szybisz, Phys. Rev. B **62**, 3986 (2000).
[32] The values of the surface grandpotential when $1/n$ tends to zero are obtained from polynomial expansions in powers of $1/n$ of

the calculated energy per particle e, chemical potential μ, and surface grandpotential σ, see Ref. 33 for a thorough discussion.
[33] L. Szybisz, J. Low Temp. Phys. **116**, 215 (1999).
[34] L. Szybisz, Phys. Rev. B **67**, 132505 (2003).
[35] M. Boninsegni, M.W. Cole, and F. Toigo, Phys. Rev. Lett. **83**, 2002 (1999).
[36] R. Mayol, M. Barranco, E.S. Hernández, M. Pi, and M. Guilleumas, Phys. Rev. Lett. **90**, 185301 (2003).
[37] D. Ross, J.E. Rutledge, and P. Taborek, Phys. Rev. Lett. **76**, 2350 (1996).
[38] M. Barranco, M. Guilleumas, M. Pi, and D.M. Jezek, in *Advances in Quantum Many-Body Theory* edited by E. Krotschek and J. Navarro (World Scientific, Singapore, 2002), Vol. 4, p. 319; S. Balibar, J. Low Temp. Phys. **129**, 363 (2002).
[39] J.O. Indekeu, Int. J. Mod. Phys. B **8**, 309 (1994).
[40] R. Blossey, Int. J. Mod. Phys. B **9**, 3489 (1995).